Available online at www.sciencedirect.com
SCIENCE DIRECT
Polymer 46 (2005) 1899–1904
polymer
www.elsevier.com/locate/polymer

Effect of 1-pentanol on the styrene emulsion polymerization

Chorng-Shyan Chern*, Ting-Chuan Yu

Department of Chemical Engineering, National Taiwan University of Science and Technology, Taipei 106, Taiwan, ROC

Received 2 September 2004; received in revised form 7 December 2004; accepted 13 December 2004
Available online 11 January 2005

Abstract

The influence of 1-pentanol (C_5OH) on the ST emulsion polymerization mechanisms and kinetics is investigated. The CMC of the ST emulsions first decreases rapidly and then levels off when the C_5OH concentration ([C_5OH]) increases from 0 to 72 mM. The effect of C_5OH increases to a maximum and then decreases when the SDS concentration ([SDS]) increases from 2 to 18 mM. At [SDS] = 2 mM, homogeneous nucleation controls the polymerization kinetics regardless of [C_5OH]. At [SDS] = 4 mM, the effect of [C_5OH] appears due to the transition from homogeneous nucleation to a mixed mode of particle nucleation (homogeneous nucleation and micellar nucleation) occurs when [C_5OH] increases from 0 to 72 mM. The effect of [C_5OH] is the strongest at [SDS] = 6 mM since the particle nucleation mechanisms span homogeneous nucleation (low [C_5OH]), a mixed mode of particle nucleation (homogeneous nucleation and micellar nucleation) (medium [C_5OH]) and micellar nucleation (high [C_5OH]). At [SDS] > 6 mM, in which micellar nucleation controls the polymerization kinetics, the effect of [C_5OH] decreases rapidly with increasing [SDS].

Keywords: Styrene emulsion polymerization; 1-Pentanol; Particle nucleation

1. Introduction

Styrene (ST) emulsion polymerization with the surfactant level greater than its critical micelle concentration (CMC) can be adequately predicted by the Smith–Ewart theory [1–6]. Particle nuclei are generated via the capture of free radicals by the monomer-swollen micelles. On the other hand, below the CMC, the polymerization is characterized by the homogeneous nucleation mechanism [7–11]. The water-borne oligomeric radical becomes insoluble when a critical chain length is achieved. It may thus coil up and form a particle nucleus. This is followed by the formation of stable primary particles via the limited flocculation of unstable particle nuclei and adsorption of surfactant on their particle surfaces. The number of latex particles nucleated per unit volume of water (N_p) and average number of radicals per particle (n) are the key parameters that control the polymerization kinetics. These are closely related to the environment of the polymerization system such as the concentration of micelles, the rate of generation of radicals in the aqueous phase, the transport of radicals between the aqueous phase and particles, and the level of surfactant available for stabilizing the growing particle nuclei.

Rao and Ruckenstein [12] showed that the CMC of sodium dodecyl sulfate (SDS) decreased with increasing the short-chain alcohol concentration. Similar results were also reported elsewhere [13–15]. Thus, short-chain alcohols may have a significant influence on the emulsion polymerization mechanisms and kinetics. For example, the point at which the transition from homogeneous nucleation to micellar nucleation occurs may shift to a lower surfactant concentration when the alcohol concentration increases. This would then lead to the increased N_p with the alcohol concentration when the surfactant concentration is kept at a constant level above the CMC. The objective of this work was to study the role of 1-pentanol (C_5OH) in the SDS-stabilized ST emulsion polymerization.

2. Experimental

2.1. Materials

ST (Taiwan Styrene Co.), SDS (J. T. Baker), methanol

* Corresponding author. Tel.: +886 2 2737 6649; fax: +886 2 2737 6644.
E-mail address: chern@ch.ntust.edu.tw (C.-S. Chern).

0032-3861/$ - see front matter © 2004 Elsevier Ltd. All rights reserved.
doi:10.1016/j.polymer.2004.12.034

(Acros), C_5OH (Janssen Chimica), sodium persulfate (Riedel-de Haen), sodium bicarbonate (Janssen Chimica), hydroquinone (Nacalia Tesque), sodium chloride (J. T. Baker), magnesium sulfate (Yakuri), a series of polystyrene standards for GPC calibration (Shodex), tetrahydrofuran (THF; Merk), nitrogen (Ching-Feng-Harng Co.), and deionized water (Barnsted Nanopure Ultrapure Water System, specific conductance $<0.057\ \mu S\ cm^{-1}$) were used in this work. ST was distilled at 40 °C under reduced pressure. All other chemicals were used as received.

2.2. Experimental methods

The CMC values of SDS for the emulsions comprising 1.7 M ST, 2.66 mM $NaHCO_3$ and various concentrations of C_5OH were determined by the electric conductance technique (Orion, Model 115) [16–18]. The emulsion was stirred using a 45°-pitched 4-bladed agitator at 250 rpm for 1 h. Note that the emulsion at the time of the conductivity measurement was kinetically stable. Furthermore, the mechanical agitation resulted in some fluctuation in the conductivity reading. Thus, 1 min before the start of measurement, the agitation was stopped and the average of three measurements at 0.5, 1 and 1.5 min was reported as the conductivity (κ). The above procedure was repeated for different concentrations of SDS ([SDS]). The CMC was then determined from the break of the slope on the κ versus [SDS] curve. This method gave satisfactory reproducibility of the CMC data.

Batch emulsion polymerization initiated by 2.58 mM sodium persulfate was carried out in a 750 ml reactor equipped with a 45°-pitched 4-bladed agitator, a thermometer, and a reflux condenser. The reaction mixture was purged with N_2 to remove the dissolved O_2 for 45 min before the start of polymerization. The temperature was controlled within the range of 70 ± 0.5 °C and the agitation speed was kept constant at 250 rpm throughout the reaction. The total solid content of the latex product is about 15% for complete monomer conversion. The product was filtered through 40-mesh (0.42 mm) and 200-mesh (0.074 mm) screens in series to collect filterable solids. Scraps adhering to the agitator, thermometer, and reactor wall were also collected. The total solid content and conversion of ST (X) were determined gravimetrically. The weight-average particle diameter (d_w), volume-average particle diameter (d_v) and polydispersity index of the particle size distribution [PDI (PSD) $= d_w/d_n$] were measured by transmission electron microscopy (TEM, JEOL TEM-1200 EXII). The parameter d_n is the number-average particle diameter. At least 300 particles per sample were counted in the particle size measurement. Based on the d_v data, the number of particles per liter water produced at the end of polymerization (N_p) was calculated.

The zeta potential of the particles (ζ) was measured with the Malvern Zetamaster. The dilution solution for the sample (total solid content = 0.01%) was 0.01 M NaCl. The reported ζ data represent an average of at least five measurements. Latex particles were precipitated by an excess of methanol, followed by thorough washes with methanol and water to remove residual SDS, C_5OH and other impurities. The weight-average polymer molecular weight (M_w) and polydispersity index of the molecular weight distribution [PDI (MWD) $= M_w/M_n$] were determined by gel permeation chromatography (GPC; Waters 515/2410/Styragel HR2, HR4, and HR6) calibrated by a series of polystyrene standards (Shodex). M_n is the number-average molecular weight.

3. Results and discussion

Representative κ versus [SDS] data are shown in Fig. 1. The CMC of the aqueous solution of SDS and 2.66 mM $NaHCO_3$ is 8.30 mM, which is very close to those of the aqueous SDS solutions in the absence of $NaHCO_3$ [19,20]. Incorporating 72 mM C_5OH into the aqueous solution of SDS and $NaHCO_3$ reduces the CMC to 4.04 mM. This can be explained by the concept of solubility parameter (δ). The closer the two δ values is, the stronger the interaction between the pair of molecules is. The values of δ for H_2O, SDS and C_5OH are 47.9, 28.8 and 22.3 $J^{1/2}\ cm^{-3/2}$, respectively [21,22]. Thus, C_5OH tends to be associated with SDS via the hydrophobic interaction in the three-component mixture. This will then result in the decrease of the water solubility of SDS (i.e., CMC). Furthermore, the presence of 1.7 M ST does not change the CMC very much because the total monomer droplet surface area is not large enough to adsorb SDS to an appreciable extent. Fig. 2 shows the CMC data as a function of the concentration of C_5OH ([C_5OH]), in which the concentrations of $NaHCO_3$ and ST were kept constant at 2.66 mM and 1.7 M, respectively. The CMC of the emulsions first decreases rapidly and then levels off when [C_5OH] increases from 0 to 72 mM.

Representative X versus time (t) curves for the ST

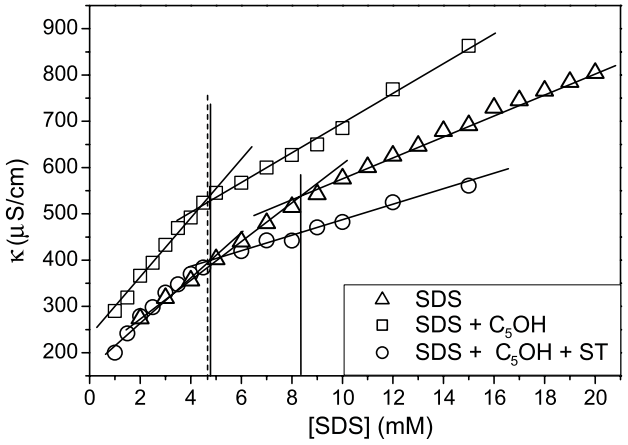

Fig. 1. Specific conductivity of SDS as a function of the bulk SDS concentration. (△) SDS, (□) SDS +72 mM C_5OH, (○) SDS +72 mM C_5OH +1.7 M ST.

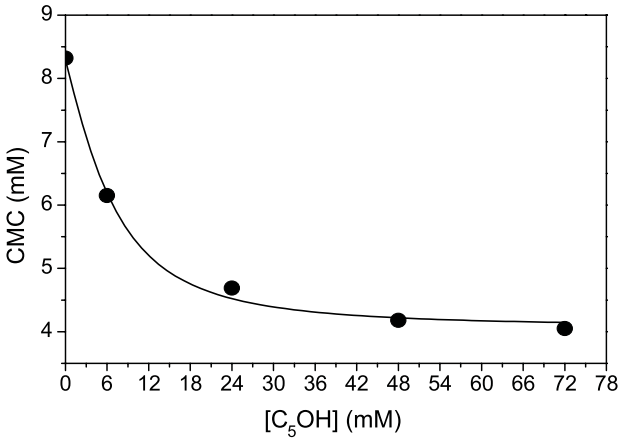

Fig. 2. Critical micelle concentration of SDS as a function of the bulk C_5OH concentration for the emulsions containing 2.66 mM $NaHCO_3$ and 1.7 M ST.

emulsion polymerizations with different [C_5OH] and [SDS] are shown in Fig. 3. The correlation between the polymerization rate ($R_p = [M]_0 dX/dt$) and [C_5OH] for the runs with [SDS] = 6 mM is $R_p \sim [C_5OH]^{0.40}$ [coefficient of determination (r^2) = 0.987, Fig. 4(a)]. $[M]_0$ is the initial monomer concentration based on total water (1.7 M) and the value of dX/dt is obtained from the least-squares-best-fitted slope of the linear portion of the X versus t curve. The exponent ω in the relationship $R_p \sim [C_5OH]^{\omega}$ versus [SDS] data are shown in Fig. 4(b). The effect of [C_5OH] on the polymerization kinetics is insignificant when [SDS] (e.g., 2 mM) is far below the CMC (Figs. 2 and 3(a)). This is most likely due to the fact that R_p is linearly proportional to the product of the number of reaction loci (N_p) and the average number of free radicals per particle (n). N_p is primarily determined by the amount of SDS available for stabilizing the particles generated by homogeneous nucleation. At [SDS] = 2 mM, N_p increases from 9.87×10^{15} to 1.38×10^{16} dm^{-3} when [C_5OH] increases from 0 to 72 mM (see the square data points in Fig. 5; $N_p \sim [C_5OH]^{0.09}$, $r^2 = 0.755$). On the other hand, n decreases from 1.19 to 0.82 when [C_5OH] increases from 0 to 72 mM (see the square data points in Fig. 6). The effects of N_p and n on the polymerization kinetics counterbalance with each other and, therefore, R_p does not vary to a significant extent as [C_5OH] is increased. At [SDS] = 4 mM, the influence of [C_5OH] floats through the transition from homogeneous nucleation ($0 <$ [C_5OH] (mM) < 24 and $8.3 >$ CMC (mM) > 4.6) to a mixed mode of particle nucleation (homogeneous nucleation and micellar nucleation) ($24 <$ [C_5OH] < 72 and $4.6 >$ CMC > 4.0) (Figs. 2–4). At [SDS] = 6 mM, C_5OH has the most significant effect because the particle formation

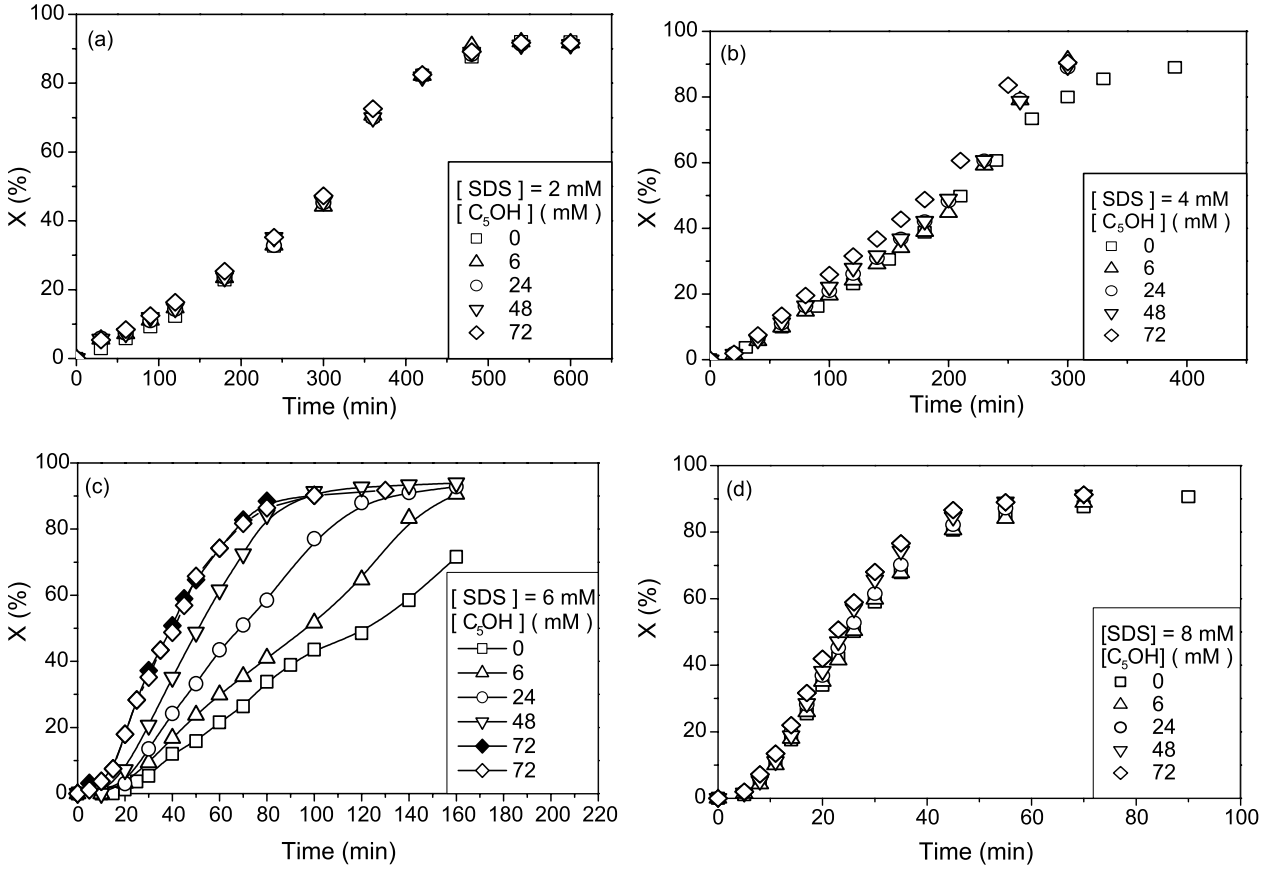

Fig. 3. Conversion as a function of time for the ST emulsion polymerizations with various bulk C_5OH concentrations. [C_5OH] (mM) = (□) 0, (△) 6, (○) 24, (▽), 48, (◇, ◆) 72. [SDS] (mM) = (a) 2, (b) 4, (c) 6, (d) 8.

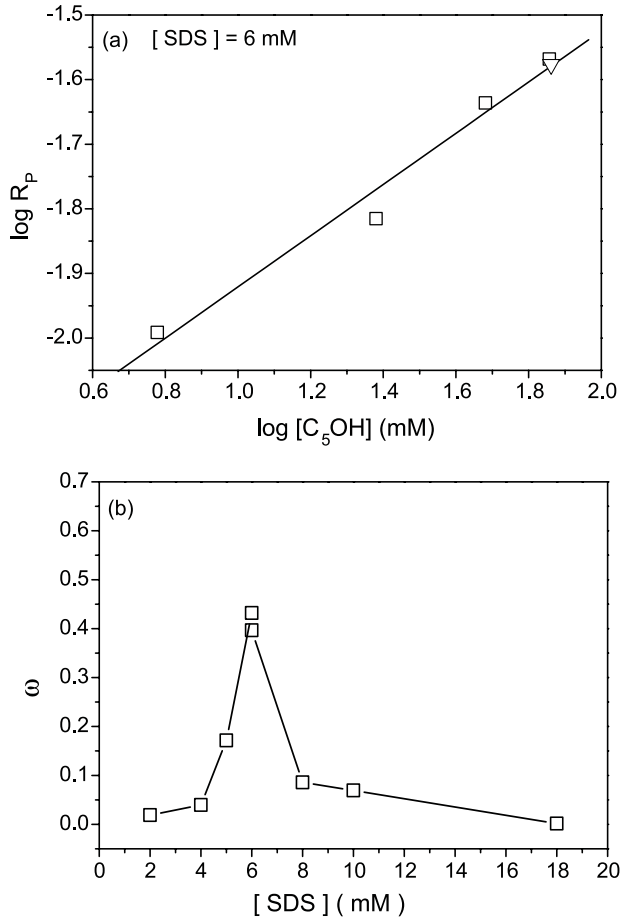

Fig. 4. (a) Logarithm plot of the polymerization rate as a function of the bulk C_5OH concentration at [SDS] = 6 mM and (b) the exponent ω in the relationship $R_p \sim [C_5OH]^{\omega}$ as a function of [SDS].

mechanisms span homogeneous nucleation ([C_5OH] < 6 mM), a mixed mode of particle nucleation ([C_5OH] = 6 mM) and micellar nucleation ([C_5OH] > 6 mM). Under the circumstances, N_p and, consequently, R_p increase

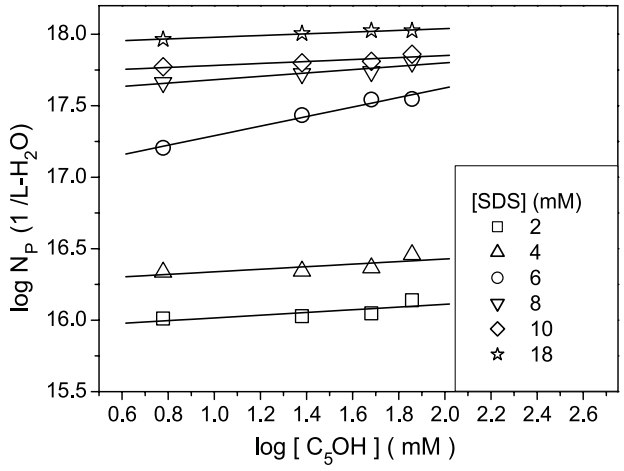

Fig. 5. Logarithm plot of the number of latex particles per unit volume of water as a function of the bulk C_5OH concentration. [SDS] (mM) = (□) 2, (△) 4, (○) 6, (▽) 8, (◇) 10, (⋆) 18.

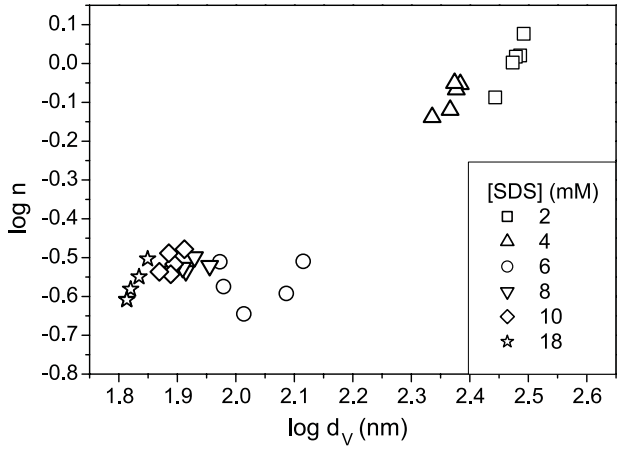

Fig. 6. Logarithm plot of the average number of free radicals per particle as a function of the volume-average particle diameter. [SDS] (mM) = (□) 2, (△) 4, (○) 6, (▽) 8, (◇) 10, (⋆) 18.

rapidly with increasing [C_5OH]. However, the effect of [C_5OH] decreases rapidly with increasing [SDS] for the polymerizations with [SDS] > 6 mM. This is attributed to the much larger number of micelles available for particle nucleation compared to the number of reaction loci (N_p) produced during polymerization. Thus, homogeneous nucleation (if present) does not play an important role in the polymerization kinetics any more.

The resultant particle size distribution is quite narrow [PDI (PSD) < 1.04] for all the polymerizations investigated and, as expected, PDI (PSD) increases slightly with increasing [SDS] (data not shown here). Fig. 6 shows the log n versus log d_v data. The n data were obtained from the relationship $n = R_p N_a / k_p [M]_p N_p$, where N_a is Avogadro number, $k_p [= 4.27 \times 10^7 \exp(-32510/RT)\ dm^3\ mol^{-1}\ s^{-1}]$ [23] the propagation rate constant, R the gas constant, and $[M]_p$ (5.2 M [24]) the concentration of monomer in the particles during the constant R_p period. Note that the presence of C_5OH results in a reduction in $[M]_p$ and, thereby, might underestimate n. Guo et al. [25] showed that the fraction of C_5OH partitioned among the various phases of the ST microemulsion in decreasing order is the interface ≫ oil phase (ca. 10 wt%) > aqueous phase. Assuming that this partitioning behavior is valid in ST emulsion polymerization, the effect of C_5OH only causes about 1% increase of n and, therefore, it is not taken into account in this work. At constant [SDS], n increases with increasing d_v due to the decreased probability for radicals to desorb out of the particles or terminate within the particles. It is also interesting to note that a (local) minimum seems to exist in the log n versus log d_v plot and, more specifically, it occurs in the series of polymerizations with [SDS] = 6 mM and various levels of [C_5OH] (see the circular data points in Fig. 6). Although the reaction mechanisms responsible for this phenomenon are not clear at this point of time, it should be closely related to the quite complicated particle nucleation mechanisms (i.e., homogeneous nucleation ([C_5OH] < 6 mM), a mixed mode of

Table 1
Theoretical value of the radical desorption rate coefficient and some experimental data obtained from the literature for ST emulsion polymerization

Research group	T (°C)	k'_{des} ($cm^2\ s^{-1}$)	References
Theory	60	6.0×10^{-12}	[26,27]
Hansen and Ugelstad	60	3.9×10^{-14}	[28]
Nomura et al.	50	$(4.3\pm2.9)\times10^{-13}$	[29]
Gilbert and Napper	60	4.8×10^{-13}	[30]
Lee and Poehlein	60	$(5.3\pm1.8)\times10^{-13}$	[31]
Chern and Lee	60–80	$1.30\times10^{-7}\exp(-34310/RT)$	[32]
This work	70	$(2.2\pm1.0)\times10^{-11}$	

particle nucleation ([C_5OH] = 6 mM) and micellar nucleation ([C_5OH] > 6 mM)) involved in the polymerization system. Further research is required to clarify this postulation. Furthermore, all the n data are smaller than 0.5 except the polymerizations with [SDS] ≦4 mM. This implies that desorption of radicals is a key factor that controls the polymerization kinetics. Desorption of radicals involves the chain transfer of a polymeric radical to ST, which results in a small and rather mobile ST radical. This is followed by the diffusion of this ST radical from the interior of a particle, across the particle-water interface, and then into the aqueous phase. The radical desorption reduces n and, thereby, decreases R_p.

Nomura et al. [26,27] derived a theoretical equation to predict the radical desorption rate coefficient (k'_{des}). Table 1 lists the theoretical value of k'_{des} at 60 °C and some experimental data obtained from ST emulsion polymerization. Apparently, our knowledge about the radical desorption is rather limited, as shown by the deviation of the k'_{des} data from the theoretical prediction and the scattered k'_{des} data at 60 °C. The following empirical equation was used in this work to estimate k'_{des} at 70 °C when $n \leqq 0.5$ [26].

$$n = 1/2\,\{-\alpha'/m + [(\alpha'/m)^2 + 2\alpha'/m]^{1/2}\} \quad (1)$$

where α' [$=\rho_i v_p/(k_t N_p)$] is the dimensionless group associated with the absorption of radicals by the particles, m ($=k_{des}v_p/k_t$) is the dimensionless group associated with the desorption of radicals out of the particles, ρ_i is equal to $2fk_d[I]$, f is the initiator efficiency factor, k_d [$=6.06\times10^{16}\exp(-140167/RT)\ s^{-1}$] [33] is the initiator decomposition rate constant, v_p is the volume of a particle, k_t [$=8.2\times10^9\exp(-14510/RT)\ dm^3\ mol^{-1}\ s^{-1}$] [34] is the termination rate constant, and k_{des} [$=k'_{des}/(v_p)^{2/3}$] [31] is the desorption rate constant. With the knowledge of n and α', the values of m (i.e., k_{des} or k'_{des}) at 70 °C and different [SDS] and [C_5OH] can thus be determined (Table 1). The values of k'_{des} obtained from this study are quite high compared to the literature data. This is most likely due to the presence of C_5OH that enhances the radical desorption rate. The C_5OH radical originating from the chain transfer of a polymeric radical to C_5OH is more water-soluble and, hence, it shows a stronger tendency to desorb out of the particle in comparison with the ST radical.

Fig. 7(a) shows that M_w increases with increasing [SDS]. This is attributed to the enhanced radical segregation effect (i.e., increased N_p) with [SDS] (Fig. 5). At constant [SDS], the molecular weight distribution becomes narrower when [C_5OH] increases from 0 to 72 mM, but this effect decreases with increasing [SDS] (Fig. 7(b)). Finally, the ζ versus [SDS]/($\pi d_v^2 N_p$)) (i.e., surface charge density) data for the polymerizations with different [SDS] and [C_5OH] are shown in Fig. 8. As expected, at constant [SDS], ζ increases with increasing surface charge density. It is the surfactant loading and the C_5OH-regulated particle nucleation that control the electrophoresis properties of the colloidal particles. These molecular weight and zeta potential data

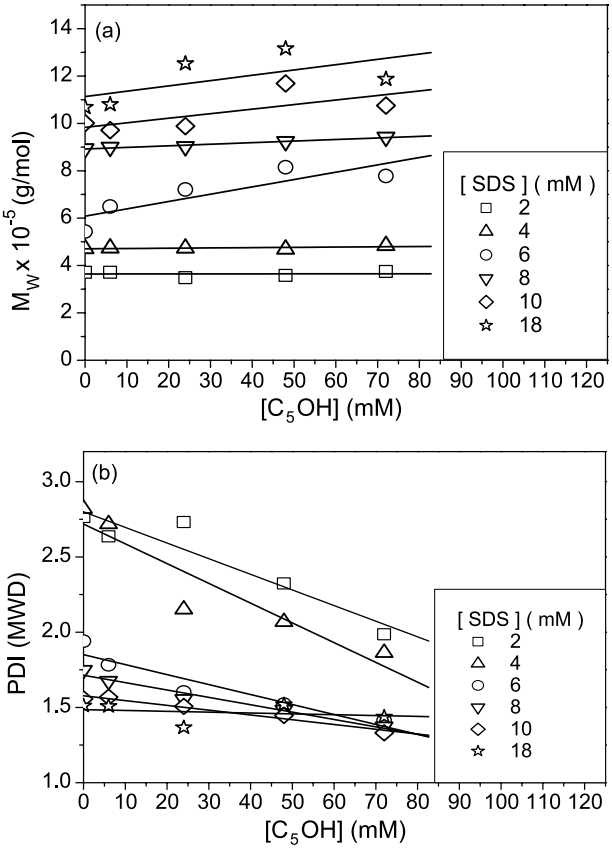

Fig. 7. (a) Weight-average molecular weight and (b) polydispersity index of the molecular weight distribution as a function of the bulk C_5OH concentration. [SDS] (mM) = (□) 2, (△) 4, (○) 6, (▽) 8, (◇) 10, (★) 18.

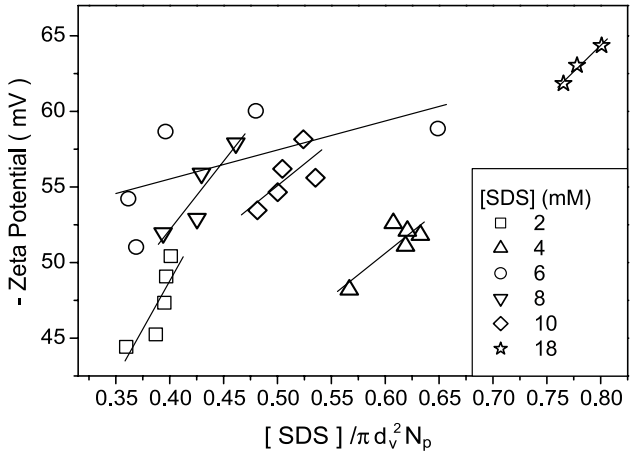

Fig. 8. Zeta potential of latex particles as a function of the surface charge density. [SDS] (mM) = (□) 2, (△) 4, (○) 6, (▽) 8, (◇) 10, (⋆) 18.

provide supporting evidence for the important role of C_5OH in the ST emulsion polymerization kinetics.

4. Conclusions

The influence of C_5OH on the ST emulsion polymerization mechanisms and kinetics is significant. This is due to the depression of the CMC values of the SDS-stabilized ST emulsions by C_5OH. The CMC of the emulsions first decreases rapidly and then levels off when the C_5OH concentration ([C_5OH]) increases from 0 to 72 mM. The effect of C_5OH increases to a maximum and then decreases when the SDS concentration ([SDS]) increases from 2 to 18 mM. At [SDS] = 2 mM, homogeneous nucleation controls the polymerization kinetics regardless of [C_5OH] because there are no micelles available for particle nucleation. At [SDS] = 4 mM, the effect of [C_5OH] appears because the transition from homogeneous nucleation to a mixed mode of particle nucleation (homogeneous nucleation and micellar nucleation) occurs when [C_5OH] increases from 0 to 72 mM. The effect of [C_5OH] is the strongest at [SDS] = 6 mM since the particle nucleation mechanisms span homogeneous nucleation (low [C_5OH]), a mixed mode of particle nucleation (homogeneous nucleation and micellar nucleation) (medium [C_5OH]) and micellar nucleation (high [C_5OH]). However, the effect of [C_5OH] decreases rapidly with increasing [SDS] for the polymerizations with [SDS] $>$ 6 mM. This is attributed to the much larger number of micelles available for particle nucleation compared to the number of reaction loci (N_p) generated during polymerization. Desorption of radicals out of the particles plays an important role in the polymerization kinetics except the runs with [SDS] $\leqq$ 4 mM. The average desorption rate constant at 70 °C obtained from this work is $(2.2 \pm 1.0) \times 10^{-11}$ $cm^2\ s^{-1}$. The polymer molecular weight and zeta potential data provide supporting evidence for the important role of C_5OH in the ST emulsion polymerization kinetics.

References

[1] Harkins WD. J Chem Phys 1945;13:381.
[2] Harkins WD. J Chem Phys 1946;14:47.
[3] Harkins WD. J Am Chem Soc 1947;69:1428.
[4] Smith WV. J Am Chem Soc 1948;70:3695.
[5] Smith WV, Ewart RH. J Chem Phys 1948;16:592.
[6] Smith WV. J Am Chem Soc 1949;71:4077.
[7] Priest WJ. J Phys Chem 1952;56:1977.
[8] Roe CP. Ind Eng Chem 1968;60:20.
[9] Fitch RM, Tsai CH. Polymer colloids. In: Fitch RM, editor. New York: Plenum Press; 1971. p. 73.
[10] Fitch RM, Tsai CH. Polymer colloids. In: Fitch RM, editor. New York: Plenum Press; 1971. p. 103.
[11] Fitch RM. Br Polym J 1973;5:467.
[12] Rao IV, Ruckenstein E. J Colloid Interface Sci 1986;113:375.
[13] Benito I, Garcia MA, Monge C, Saz JM, Marina ML. Colloids Surf A 1997;125:221.
[14] Chauhan MS, Kumar G, Kumar A, Chauhan S. Colloids Surf A 2000; 166:51.
[15] Romani AP, Gehlen MH, Lima GAR, Quina FH. J Colloid Interface Sci 2001;240:335.
[16] Goddard ED, Benson GC. Can J Chem 1957;35:986.
[17] Mukerjee P, Mysels KJ, Dulin CI. J Phys Chem 1958;62:1390.
[18] Chang HC, Lin YY, Chern CS, Lin SY. Langmuir 1998;14:6632.
[19] Hayase K, Hayano S. Bull Chem Soc Jpn 1977;50:83.
[20] Jain AK, Singh RPB. J Colloid Interface Sci 1981;81:536.
[21] Barton AFM. CRC handbook of solubility parameter and other cohesion parameters. CRC Press: Boca Raton, FL; 1983.
[22] Brandrup J, Immergut EH, editors Polymer handbook. 3rd ed. New York: Wiley; 1989.
[23] Gilbert RG. Pure Appl Chem 1996;68:1491.
[24] Bartholome E, Gerrens H, Herbeck R, Weitz HM. Z Elektrochem 1956;60:334.
[25] Guo JS, El-Aasser MS, Sudol ED, Yue HJ, Vanderhoff JW. J Colloid Interface Sci 1990;140:175.
[26] Nomura M. Emulsion polymerization. In: Piirma I, editor. New York: Academic; 1982. p. 191.
[27] Nomura M, Harada M, Nakagawara K, Eguchi W, Nagata S. J Chem Eng Jpn 1971;4:160.
[28] Hansen FK, Ugelstad J. J Polym Sci Polym Chem Ed 1979;17:3047.
[29] Nomura M, Yamamoto K, Horie I, Fujita K. J Appl Polym Sci 1982; 27:2483.
[30] Gilbert RG, Napper DH. J Macromol Sci Rev Macromol Chem Phys 1983;C23:127.
[31] Lee HC, Poehlein GW. Polym Process Eng 1987;5:37.
[32] Chern CS, Lee C. J Polym Sci Polym Chem Ed 2002;40:1608.
[33] Kolthoff IM, Miller IK. J Am Chem Soc 1951;73:3055.
[34] Matheson MS, Auer EE, Bevilacqua EB, Hart EJ. J Am Chem Soc 1951;73:1700.